Experimental characterisation of a Fresnel lens photovoltaic concentrating system

Yupeng Wu [a,*], Philip Eames [b], Tapas Mallick [c], Mohamed Sabry [d]

[a] *Department of Architecture & Built Environment, Faculty of Engineering, University of Nottingham, Nottingham NG7 2RD, UK*
[b] *Centre for Renewable Energy Systems Technology, Department of Electronic and Electrical Engineering, Loughborough University, Loughborough LE11 3TU, UK*
[c] *Department of Mechanical Engineering, School of Engineering and Physical Sciences, Heriot-Watt University, Edinburgh EH14 4AS, UK*
[d] *Solar Physics Lab, National Research Institute of Astronomy and Geophysics, Helwan, Cairo, Egypt*

Abstract

An extensive indoor experimental characterisation program to investigate the heat loss from a point focus Fresnel lens PV Concentrator (FPVC) with a concentration ratio of 100× was performed for a range of simulated solar radiation intensities between 200 and 1000 W/m^2, different ambient air temperatures, and natural and forced convection. From the experimental program it was found that the solar cell temperature increased proportionally with the increase in simulated solar radiation for all experimental tests, indicating that conductive and convective heat transfer were significantly larger than the long wave radiative heat transfer within and from the FPVC system. For the simulated worst case scenario, in which the FPVC system was tested under a simulated solar radiation intensity of 1000 W/m^2 and ambient air temperature of 50 °C with no forced convection, the predicted silicon solar cell efficiency in the FPVC system was reduced to approximately half that at standard test conditions.
© 2011 Elsevier Ltd. Open access under CC BY license.

Keywords: Fresnel lens PV Concentrator; Natural and forced convection; Thermal characterisation

1. Introduction

PV concentrator systems reduce the area of photovoltaic cells required, increase the solar radiation intensity on the photovoltaic cells and can lead to a reduction in total system cost, if the cost of the concentrator and tracking assembly are less than that of the area of photovoltaic cells displaced (Rabl, 1976; Winston et al., 2005). PV concentrators can employ reflective or refractive optical approaches or a combination of both. The two main types are (i) those that use mirrors such as a parabolic trough, parabolic dish or compound parabolic reflector, and (ii) those that use lenses such as a Fresnel lens. A reflector based concentrator requires larger areas of reflecting surface compared to the actual aperture area over which solar radiation is collected, in comparison Fresnel lens concentrators require the Fresnel lens area to match the aperture area and may be more suitable for concentrating PV applications (Singh et al., 1999). A Fresnel lens is a flat or curved optical component which focuses light by means of a series of concentric grooves (point focus) or parallel grooves (line focus), which are prismatic in section. For the point focus lens the acting angles of the prisms increase ring by ring from the centre. The light passing through each prism is refracted at a slightly different angle and focuses on a point (Al-Jumaily and Al-Kaysi, 1998). The Fresnel lens can achieve a high

* Corresponding author. Tel.: +44 (0) 115 74 84011.
  E-mail addresses: Yupeng.Wu@nottingham.ac.uk, jackwuyp@googlemail.com (Y. Wu).
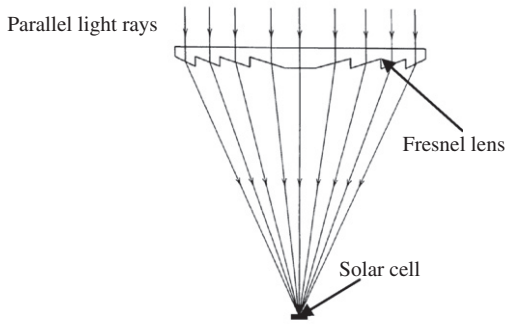
Fig. 1. A schematic diagram of a Fresnel lens PV Concentrator (Ryu et al., 2006).

energy flux with geometric concentrations ratio from 10 to over 500 being common, however, tracking systems are required and direct radiation only is concentrated. A schematic sketch of a point focus Fresnel lens PV Concentrator is presented in Fig. 1 and illustrates how a Fresnel lens can focus sunlight onto a small area.

A range of companies are currently developing Fresnel lens PV Concentrator (FPVC) systems due to their ability to increase the solar radiation intensity on the solar cells to high levels, simultaneously, the housing of the FPVC system performing as a heat sink and enhancing heat transfer from the solar cells to the ambient environment. Salim and Eugenio (1990) reported the performance of a 350 kW Fresnel lens PV Concentrator system located about 45 km northwest of Riyadh, the capital city of Saudi Arabia. They concluded that this PV system was a reliable source of

power with minimum operation and maintenance requirements. Whitfield et al. (1999) undertook experimental tests for a two-axis tracking point-focus Fresnel lenses PV Concentrator with a concentration ratio of 32×. During a continuous 12 h outdoor test at Reading UK, on the 8th of August 1998, the Fresnel lens PV Concentrator system generated 505 Wh of electricity. A considerable volume of research has been undertaken and reported in the literature aimed at improving the optical efficiency of the Fresnel lens and at optimising the Fresnel lens design to provide a uniform radiation intensity distribution over the solar cell surface (Ryu et al., 2006; Nabelek et al., 1991; Andreev et al., 2004; Mallick and Eames, 2007a). To date, however, few have studied the thermal behaviour of FPVC systems (Mallick and Eames, 2007b), however, the thermal management of a concentrating PV system, especially when using crystalline silicon solar cells is crucial. The mechanisms which can be used to moderate cell temperature rise include increasing system heat dissipating areas (utilising fins), passive cooling (natural ventilation) and active cooling (forced convection of air over the front and rear of the cells or water circulation at the rear of the cell allowing solar thermal collection also if required). An extensive indoor experimental program to characterise the heat loss from a typical point focus Fresnel lens PV Concentrator has been undertaken for a range of simulated solar radiation intensities, different ambient air temperatures, and both natural and forced convection. The experimentally analysed FPVC with a design concentration ratio of 100× is illustrated schematically in Fig. 2. The 1000 mm long V-trough that forms the housing of the concentrator system is made from
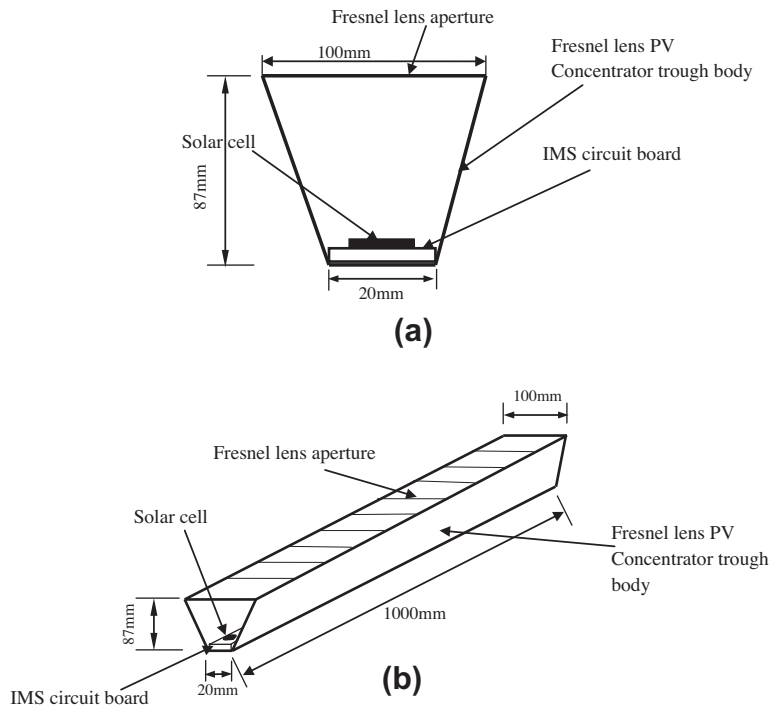

Fig. 2. (a) Cross sectional view of the experimentally characterised FPVC system and (b) 3D diagram of the experimentally characterised FPVC system.

aluminium with a wall thickness of 0.6 mm. The V-trough aperture is 100 mm wide tapering to a base width of 20 mm, the height of the trough is 87 mm. In operation ten solar cells with dimensions of 12 mm long by 10 mm wide are installed on a 1000 mm long, 1.5 mm thick 20 mm wide Insulated Metal Substrate (IMS) circuit board mounted at the base of the FPVC housing.

2. Design and selection of the experimental test facilities

To enable the experimental tests to be easily repeatable, the Fresnel lens PV Concentrator (FPVC) was tested inside a heated insulated enclosure which was used to maintain a constant environmental temperature. Ten Electrical Resistance Heaters (ERHs), similar in dimension to the solar cells used in the FPVC system, replaced the solar cells, and were used to simulate the heat generated at the solar cells in the FPVC system when exposed to direct solar radiation. The small amount of solar radiation which is absorbed by a Fresnel lens when exposed to direct solar radiation was considered to be negligible and was not simulated. Initially, the solar cell conversion efficiency was assumed constant at 15% in all tests.

2.1. Selection of the Electrical Resistance Heaters (ERHs)

The heat to be dissipated from a solar cell in the Fresnel lens PV Concentrator was determined using the following equation:

$$Q = A \cdot I \cdot \eta_{opt} \cdot (1 - \eta_{PV}) \quad (1)$$

where A is the area of the Fresnel lens, I is the incident solar radiation intensity, η_{opt} is the optical efficiency of the FPVC system and η_{PV} is the solar-electrical conversion efficiency.

After assuming that the maximum incident beam solar radiation intensity on the FPVC aperture was 1000 W/m², the optical efficiency of the FPVC system was 85% (Andreev et al., 2004) and the electrical conversion efficiency of the solar cell was 15%. From Eq. (1), it can be calculated for these conditions that each solar cell in the FPVC system would, at steady state, need to dissipate 7.225 W of heat. Ten 20 W 20 Ω ERHs, TO-126, with dimensions of 12 mm × 8 mm × 3 mm having a rated output greater than 7.225 W were selected to simulate the heat that would be dissipated from the PV cells in the FPVC system and used in the experiments. To control the power input into each of the resistance heaters a variable output power supply was used.

2.2. Design and fabrication of the temperature controlled test chamber

A thermally insulated test chamber was designed and fabricated and used to provide a constant temperature environment for the experimental characterisation of the thermal behaviour of the FPVC system. The test chamber dimen-

sions were 1500 mm long by 1400 mm wide by 1400 mm high, this provided sufficient space to install the FPVC system and incline it over a range of angles. The test chamber frame was fabricated from 30 mm × 30 mm cross section Bosch Aluminium Profiles. The floor of the chamber was comprised of a 3 mm thick aluminium base plate, onto which a 15 mm thick plywood board was bonded, the walls of the box were constructed from 15 mm thick plywood boards. Celotex insulation boards 25 mm thick with a thermal conductivity of 0.024 W/m K were bonded to the inner surface of all of the chamber walls to reduce heat loss from the inside of the test chamber to the outside ambient environment.

The first stage of the experimental test program was designed to investigate natural convective heat loss, no wind conditions. Eight 200 W PTC element enclosure heaters connected in parallel to a FTST 400 K temperature controller were used to increase the ambient temperature in the test chamber and maintain it at a predefined set point. The maximum generated heat flux on the aluminium base plate surface was set to a value of 850 W/m².

In the second stage of the experimental test program, the thermal characterisation of the FPVC system was undertaken for forced convective heat transfer, simulating windy conditions. Twelve W2E 200-HH 38-01 exhaust fans having a maximum air volume flow rate of 1030 m³/h (average air speed 5.65 m/s) and fan diameter of 200 mm were mounted onto the outer surface of the test chamber, opposite to the chamber door. The air flow rate through the fans was set using a fan speed controller.

3. Experimental apparatus setup used for indoor heat loss characterisation

3.1. Installation of the resistance heaters to the FPVC system

Ten TO-126 ERHs were connected in parallel and placed in thermal contact with the IMS circuit board on which the solar cells would normally be mounted and bonded to it at the solar cell locations using a thermally conductive adhesive. The IMS circuit board used was a heat-conducting electrically-isolating material. The adhesive had a maximum operational temperature of 150 °C and thermal conductivity of 0.815 W/m K (Anon, 2008). A double-sided tape (Technibond T555) was used to fix the IMS circuit board to the inner base of the PV concentrator unit.

3.2. Temperature measurements and full experimental test apparatus

Calibrated T type thermocouples were used to measure temperatures in the FPVC system at the locations illustrated in Fig. 3 and detailed in Table 1. A photograph of the test chamber, FPVC system, power supply and the temperature controller is presented in Fig. 4. The K type temperature sensor used by the temperature controller was
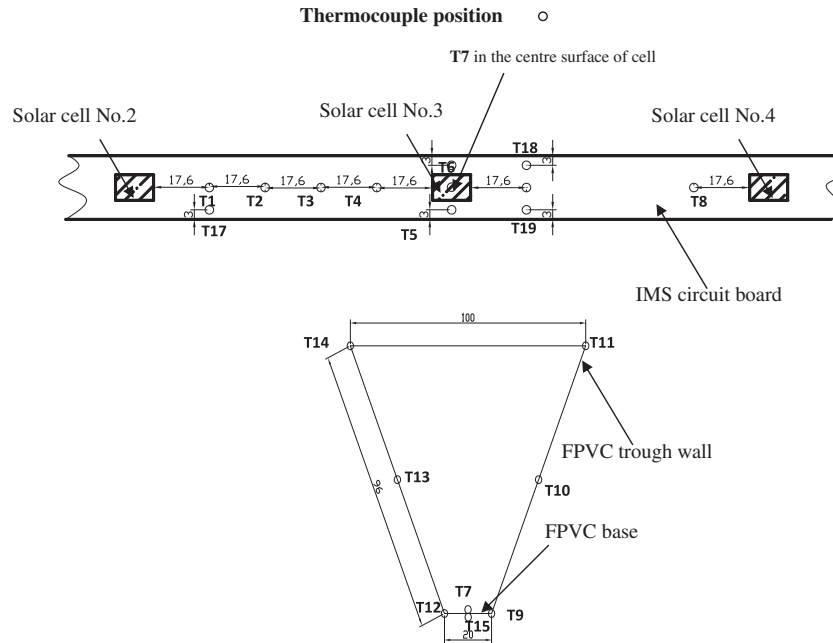
Fig. 3. Detailed view of the thermocouple locations in the FPVC system, all dimensions in mm.

Table 1
Thermocouple locations in the FPVC system and the test chamber.

Thermocouple	Thermocouple locations
T1–T4	Distributed between Nos. 2 and 3 solar cells on the IMS board
T5 and T6	On both sides of the No. 3 solar cell
T7	On the No. 3 solar cell
T8	17.6 mm from the No. 4 solar cell
T9–T14	On the FPVC long trough walls
T15	At the rear of the trough base
T16	At the same horizontal plane as the trough base used to measure the ambient air temperature shown in Fig. 4
T17	7 mm from T1
T18 and T19	7 mm from T20
T20	17.6 mm from the No. 3 solar cell

located at the same position as thermocouple 16 (T16) in Fig. 4.

4. Thermal behaviour of the FPVC system with natural convective heat transfer

4.1. Ambient temperature of 20 °C

The thermal behaviour of the FPVC system was determined for simulated solar radiation intensities at the Fresnel lens of 200, 400, 600, 800 and 1000 W/m^2 for natural convective heat loss (no wind condition) by running the heaters in both the FPVC system and the test chamber until the FPVC system reached steady state. The final ambient temperature of the test chamber was set at 20 °C by controlling the heat input from the chamber heaters. Temperature readings were taken every 30 s. For all the tests, after approximately 30 min, steady state temperatures were reached for all sensors in the FPVC system.

From the measured temperatures, isotherms at intervals of 4 °C have been plotted around the simulated No. 3 solar cell along the IMS circuit board for simulated solar radiation intensities of 200, 400, 600, 800 and 1000 W/m^2 and are presented in Fig. 5. Fig. 6 presents the temperature profile in the horizontal long central axis (X-direction) along the IMS circuit board centred on the 3rd solar cell location for solar radiation intensities of 200, 400, 600, 800 and 1000 W/m^2. From Figs. 5 and 6, it can be seen that when the simulated solar radiation intensity is 1000 W/m^2, the PV cell achieves a maximum temperate of 92.4 °C in the FPVC system, 72.4 °C higher than the ambient temperature and over 20 °C higher than those recorded on the IMS strip. The temperatures at distances $X = -23.6$ mm, 23.6 mm and 76.4 mm are all similar at approximately 70 °C, this is to be expected since they are all located at similar distances from the simulated solar cells. Temperatures at these locations are, however, approximately 3 °C higher than that measured at $X = -76.4$ mm, which is closer to the side end wall of the FPVC trough. Similar thermal behaviour and temperature distributions were found for simulated solar radiation intensities of 200, 400, 600 and 800 W/m^2. The peak temperatures on the IMS board are in the area around the cell due to heat input at this point. No significant temperature differences are measured on the IMS circuit board at distances of over 18 mm away from the simulated solar cells, this could be due to the thermal resistance between the solar cell and the IMS board.

The measured temperatures for the solar cell, the FPVC trough base rear, the bottom and the top of the FPVC trough wall and the temperature difference between the solar cell and the trough base rear are plotted in Fig. 7. The following can be observed from Fig. 7, when the ambient air temperature is 20 °C, the solar cell temperature
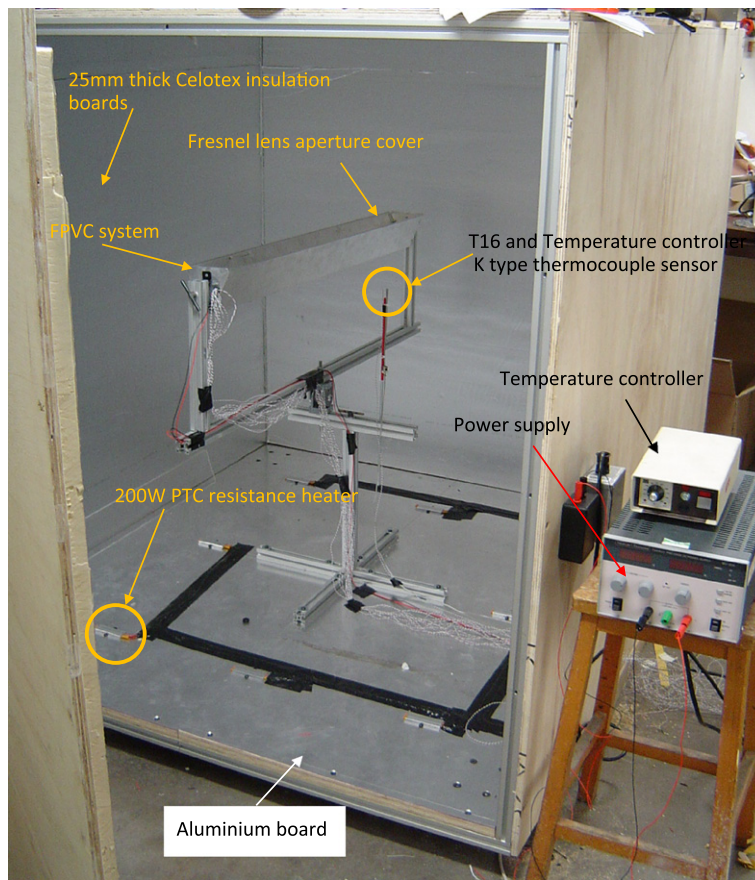
Fig. 4. A photograph of the test facility developed for the FPVC system showing the test chamber, temperature controller, power supply and the FPVC system.

linearly increases with the increase in the intensity of simulated solar radiation. Due to long-wave radiative heat transfer being a function of T^4, it can be deduced that radiative heat transfer is less than conductive and convective heat transfer in the FPVC system. When the simulated solar radiation intensity was 1000 W/m², the temperature difference between the solar cell and the trough base rear was 36.5 °C, and 7.7 °C at a simulated solar radiation intensity of 200 W/m². The measured temperature differences between the solar cell and the trough base rear are significant for the small distance between the solar cell and the rear of the trough base, and results due to the high thermal resistance between the IMS strip and the trough base. There were no significant temperature differences measured between the trough base rear and the bottom of the trough wall in all tests. The temperatures at the trough base are approximately 7 °C higher than those on the top of the trough wall for a simulated solar radiation intensity of 1000 W/m², and 2 °C higher for 200 W/m².

4.2. Ambient temperature of 50 °C

To investigate the thermal performance of the FPVC system in a hot climate, an ambient air temperature of 50 °C was maintained in the test chamber, slightly higher than the average summer ambient air temperature of 45 °C in the Arabian Gulf (Anon, 2009). This temperature was selected to investigate the probable extreme operating conditions that the system will be subjected to if installed for large scale power generation in high solar radiation areas. Simulated solar radiation intensities of 200, 400, 600, 800 and 1000 W/m² were again applied in the FPVC system and a natural convective heat loss condition used when running the heaters in both the FPVC system and the test chamber until steady state was obtained with an ambient air temperature of 50 °C.

The thermal performance of the FPVC for a 50 °C ambient air temperature with natural convection has a similar characteristic to it with 20 °C ambient air temperature. The measured temperatures of the solar cell, the FPVC trough base rear, the bottom and the top of the FPVC trough wall and the temperature difference between the solar cell and the trough base rear are plotted in Fig. 8. From Fig. 8, it can be seen that when the ambient air temperature is 50 °C, the FPVC system demonstrates similar thermal behaviour to the case for an ambient air temperature of 20 °C. The linearity of the temperature increase with input power indicates that conductive and convective heat
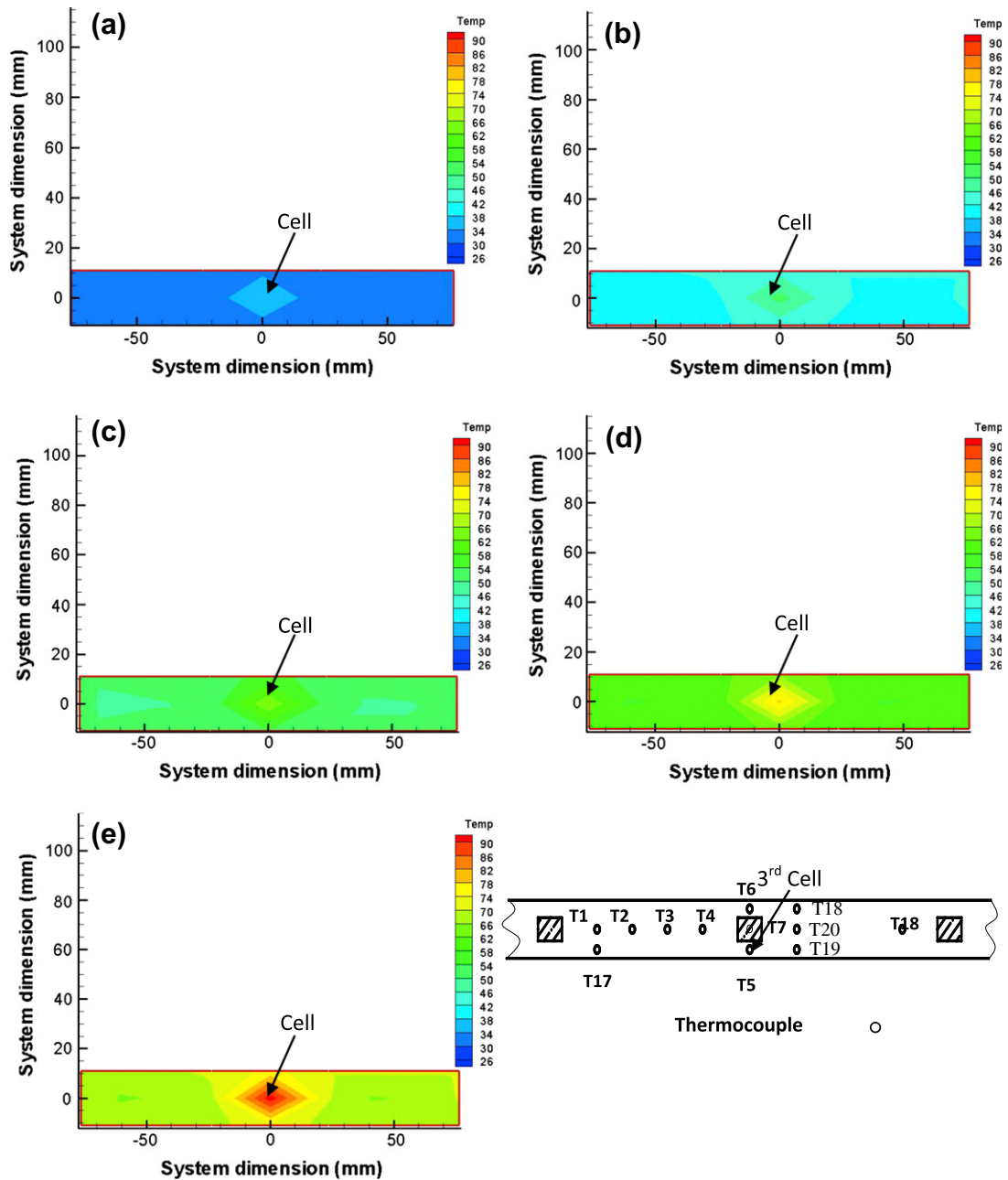
Fig. 5. Two dimensional isotherms generated from experimental measurements around the 3rd simulated solar cell on the IMS circuit board. Simulated solar radiation intensity was (a) 200, (b) 400, (c) 600, (d) 800 and (e) 1000 W/m^2 with an ambient air temperature of 20 °C.

transfers again are the dominant heat transfer mechanisms in the FPVC system. The measured temperature difference between the solar cell and the trough base rear is significant.

From Figs. 7 and 8, it can be seen that when the system was tested at different ambient air temperatures with similar simulated solar radiation intensities, the temperature differences between the cell and the ambient air temperature were similar. The temperature difference was approximately 70 °C at a simulated solar radiation intensity of 1000 W/m^2 with an ambient air temperature of 50 °C, and was 72 °C at the similar radiation intensity level with ambient air temperature of 20 °C. Both temperature differences were 17 °C for a solar radiation intensity of 200 W/m^2, and ambient air

temperatures of 20 °C and 50 °C. The measured temperature differences between the trough base rear and the ambient air temperature were also similar, when the system was tested at ambient air temperatures of 20 °C and 50 °C for the same simulated solar radiation intensities.

5. Thermal characterisation of the FPVC system with an ambient air temperature of 20 °C and forced convection heat transfer

The thermal characteristics of the FPVC were investigated for simulated solar radiation intensities of 200, 400, 600, 800 and 1000 W/m^2 with two kinds of forced convective
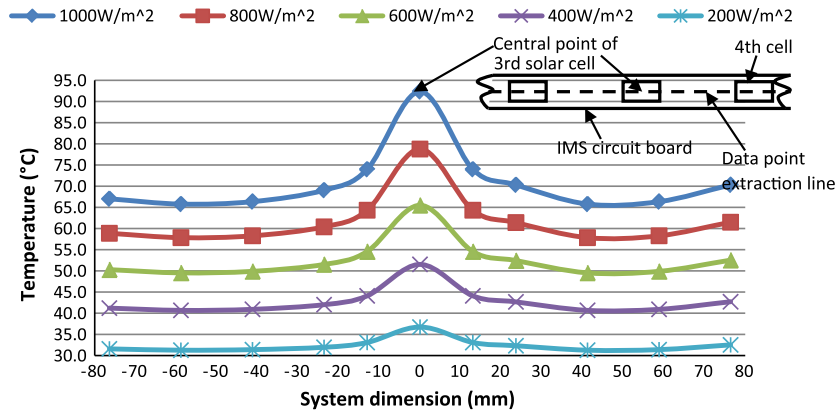
Fig. 6. Temperature distribution in the horizontal long central axis (*X*-direction) around the 3rd simulated solar cell on the IMS circuit board for solar radiation intensities of 200, 400, 600, 800 and 1000 W/m², and an ambient air temperature of 20 °C.
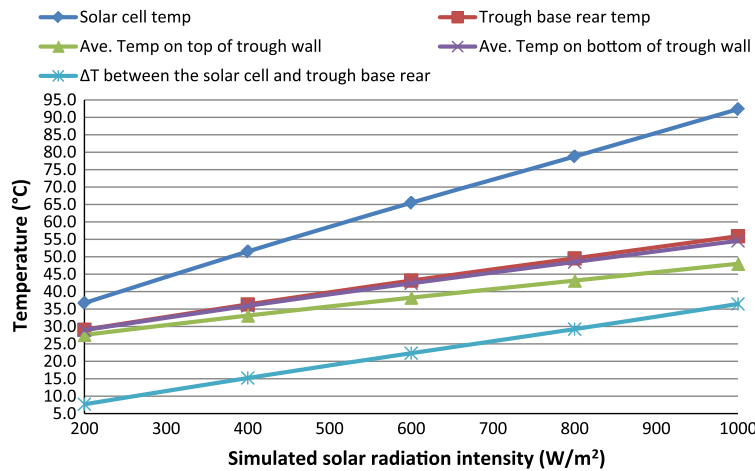

Fig. 7. The measured temperatures in the FPVC system at selected simulated solar radiation intensities with an ambient air temperature of 20 °C.
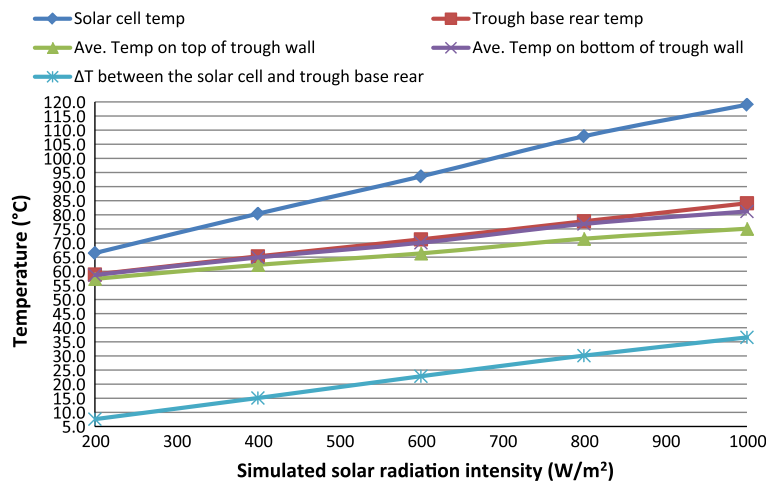

Fig. 8. The measured temperatures of the FPVC system for selected solar radiation intensities, and an ambient air temperature of 50 °C.

cooling conditions, forced air flow along the long axis and force air flow over the cross section of the FPVC system, respectively. The average air velocity of 2.0 m/s with an

ambient temperature of 20 °C was applied in the tests. Under the forced convective cooling conditions, the FPVC system demonstrated similar thermal behaviour when compared

to that at 20 °C ambient air temperature with natural convective cooling only. The measured temperatures of the No. 3 simulated solar cell and the FPVC trough base rear with solar radiation and an ambient air temperature of 20 °C under natural convection and forced convection are plotted in Fig. 9. The measured detailed temperature distribution around the No. 3 solar cells under the forced convective cooling conditions are shown in Figs. A1–A3 in Appendix A. From Fig. 9, it can be seen that the cell temperature is significantly reduced by using forced convective heat transfer when compared to that for natural convection. At an ambient temperature of 20 °C and under the natural convective conditions, the solar cell temperature is higher than that with a 2.0 m/s air flow over the FPVC system. When the air flows along the long axis of the FPVC trough, the cell temperature is only slightly higher than that measured for air flow over the cross section, possibly due to a lower convective heat transfer rate occurring at the trough surface. When the simulated solar radiation intensity was 1000 W/m², the measured cell temperature was 92.4 °C for the natural convective case, and 76.4 and 74.6 °C for forced convective case with 2.0 m/s air flow along the long axis, and over the cross section of the FPVC, respectively. The temperature of the trough base rear has a similar temperature distribution to that of the cell under natural and forced convection. All temperatures are higher for natural convection than those measured for forced convection. The temperature difference between the cell and trough base rear are similar for similar values of simulated solar radiation for both natural and forced convective conditions. When the solar radiation is 1000 W/m², the temperature difference between the cell and the trough base rear is around 38 °C, and approximately 8 °C at 200 W/m².

For the FPVC system under forced convective cooling conditions, conduction and convection are still the dominant heat transfer mechanisms in the FPVC system, illustrated by the linearity of the increase in temperature of the simulated solar cell with input power. The temperature

difference between the solar cell and the trough base rear is again significant.

6. Discussion

For crystalline silicon cells, the cell efficiency decreases by approximately 5% with a 10 °C temperature increase (Anon, 2005). The electrical conversion efficiency of the FPVC system can be calculated by the following equation:

$$\eta_{PV} = \eta_{PV.STC} \times [1 + 0.005 \times (25 - T_{cell})] \tag{2}$$

where $\eta_{PV.STC}$ is the standard test condition PV electricity conversion efficiency ($\eta_{PV.STC} = 15$).

Based on the measured solar cell temperatures in Sections 4 and 5, the electrical conversion efficiency of the 3rd cell in the FPVC system at simulated solar radiation intensities of 200 W/m², 400 W/m², 600 W/m², 800 W/m² and 1000 W/m² for different ambient air temperatures, and both natural and forced convection calculated using Eq. (2) are shown in Table 2. From Table 2, it can be seen that in the simulated worst case scenario, when the FPVC system was under natural convection (no wind conditions) at a simulated solar radiation intensity of 1000 W/m² and ambient air temperature of 50 °C, the solar cell efficiency in the FPVC system was reduced to 7.95%, for an ambient air temperature of 20 °C, it was reduced to 9.95%. When the ambient air temperature was 20 °C, the predicted efficiencies were 11.15% and 11.28% under forced air (air velocity of 2 m/s) flow along the length of the FPVC and with air flow across the cross section, respectively.

Assuming a constant cell electrical conversion efficiency of 15%, a constant fraction of the incident solar radiation would be dissipated by the solar cell for each solar radiation intensity level. From Table 2, it can be seen that for the worst scenario when the ambient temperature was 50 °C with natural convection only, the predicted cell electrical conversion efficiency would have reduced to approximately 8% rather than the 15% assumed. The energy dissipated as heat from
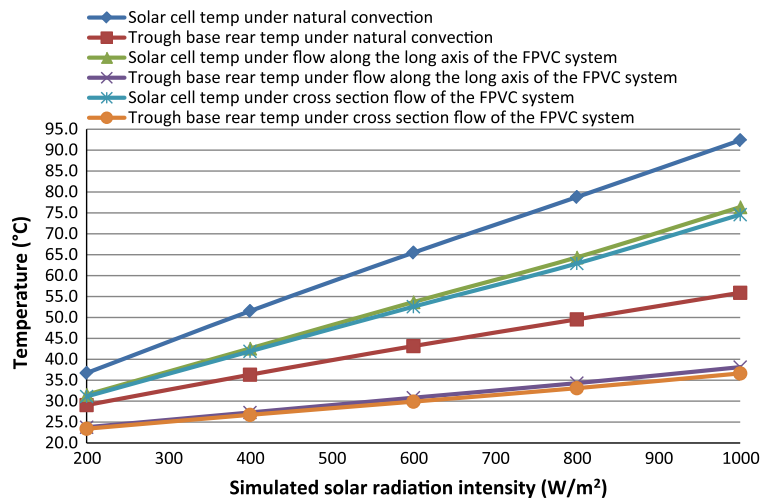

Fig. 9. The measured temperatures for the FPVC system with solar radiation and an ambient air temperature of 20 °C for natural and forced convection conditions.

Table 2
Predicted electrical conversion efficiency at simulated solar radiation intensities of 200 W/m², 400 W/m², 600 W/m², 800 W/m² and 1000 W/m² for different ambient air temperatures, and natural and forced convection.

Initial solar radiation intensities (W/m²)	Electrical conversion efficiency (%)			
	Natural convective heat transfer only		Forced convection (air velocity of 2 m/s) and ambient air temperature of 20 °C	
	Ambient temperature of 20 °C	Ambient temperature of 50 °C	Forced air flow along the long axis of the FPVC system	Forced air flow over the cross section of the FPVC system
200	14.12	11.89	14.51	14.54
400	13.01	10.85	13.68	13.73
600	11.96	9.86	12.85	12.93
800	10.97	8.79	12.05	12.16
1000	9.95	7.95	11.15	11.28

Table 3
The actual incident solar radiation intensities converted from Eq. (3).

Initial solar radiation intensities (W/m²)	Actual solar radiation intensities (W/m²)			
	Natural convective heat transfer only		Forced convection (air velocity of 2 m/s) and ambient air temperature of 20 °C	
	Ambient temperature of 20 °C	Ambient temperature of 50 °C	Forced air flow along the long axis of the FPVC system	Forced air flow over the cross section of the FPVC system
200	198	193	199	199
400	391	381	394	394
600	579	566	585	586
800	764	746	773	774
1000	944	923	957	958

the cell would thus be 7% higher. To correct for this effect the apparent insolation level should be modified using the following formula:

$$I_{act} = I \times \frac{0.85}{0.85 + d\eta} \qquad (3)$$

where I_{act} is the actual incident solar radiation intensity, $d\eta$ is solar cell efficiency difference between the initially assumed 15% and final calculated cell efficiency based on measured cell temperature.

The actual incident solar radiation intensities corresponding to the calculated solar cell conversion efficiencies are shown in Table 3. Thus for the worst case scenario the actual radiation that would lead to the temperature observed when including the reduction in efficiency due to increased temperature is 923 W. The measured solar cell temperatures at actual solar radiation intensities are illustrated in Fig. 10. The solar cell temperatures still increased linearly with the increase in the actual solar radiation in all experimental tests. It proves that the utilisation of an initial
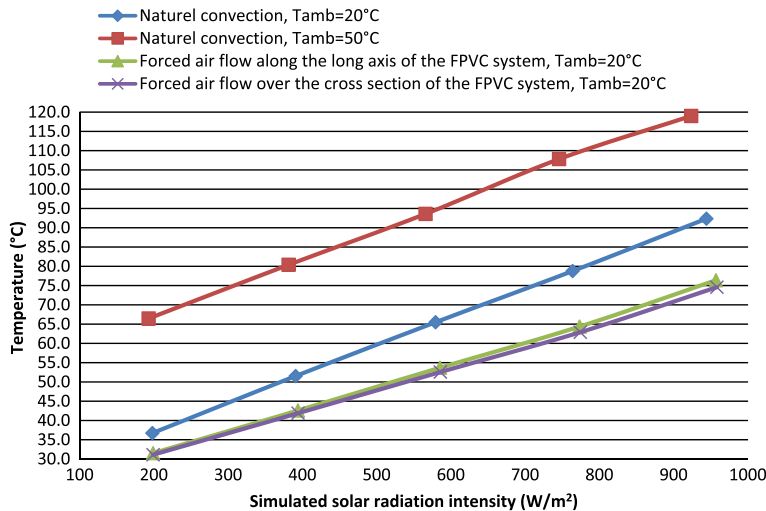

Fig. 10. The measured temperatures of No. 3 solar cell at actual incident solar radiation intensities.

constant solar cell conversion efficiency of 15% in the FPVC system does not affect the thermal behaviour of the FPVC system. The aim of this work was to examine the thermal performance of a Fresnel lens PV Concentrator system, the results and method developed can be used to both improve the design of the system and identify design limitations.

7. Conclusion and suggestions

A detailed indoor experimental characterisation of a 0.6 mm thick aluminium trough wall Fresnel lens PV Concentrator (FPVC) with a concentration ratio of 100 was undertaken at different simulated solar radiation intensities, different ambient air temperatures with natural and forced convective heat transfer conditions. The following conclusions can be drawn:

- The solar cell temperature increased linearly with the increase in the simulated solar radiation from 200 W/m^2 to 1000 W/m^2 in all experimental tests if a conversion efficiency of 15% was assumed. Conductive and convective heat transfer mechanisms were the dominant heat transfer modes within and from the FPVC system.
- The temperature differences between the solar cell and the ambient air temperatures were similar for systems tested at ambient air temperatures of 20 °C and 50 °C. The measured temperature difference between the solar cell and the trough base rear was high, and indicates high thermal resistance between the IMS board and the trough base. Temperature differences were almost the same at similar solar radiation intensities for both natural and forced air flow condition. When the solar radiation was 1000 W/m^2, the temperature difference between the solar cell and the trough base rear was around 38 °C, and approximately 8 °C at 200 W/m^2. A higher thermally conductive material should be employed between the IMS board and the trough base

rear to improve the heat transfer within the FPVC system and to dissipate heat from the solar cell and thus increase system efficiency.
- Under forced convection conditions, the solar cell temperature was significantly reduced compared to that for similar solar radiation intensities and natural convective conditions. There was no significant temperature difference between the simulated No. 3 solar cell, when tested at similar solar radiation intensities and ambient air temperatures with air flow along the long axis of the FPVC system and with air flow across the cross section.
- In the simulated worst case scenario, when the FPVC system was tested for a simulated solar radiation intensity of 1000 W/m^2, ambient air temperature of 50 °C and natural convection only, the predicted solar cell efficiency in the FPVC system was reduced from 15% to 7.95%.

From the above conclusions, the following are recommended: A three dimensional heat transfer model which simulates conduction, convection and radiation modes of heat transfer should be developed for the FPVC system which after validation can be used to more fully understand the thermal performance of the system. The thermal performance results from the simulations could be used to both improve the design of the system and identify design limitations.

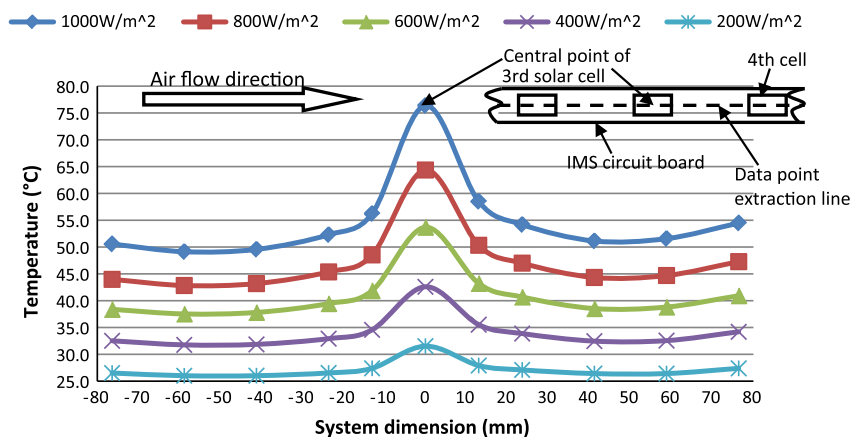## Appendix A

Figs. A1–A3.

Fig. A1. Temperature distribution in the horizontal long central axis (*X*-direction) for the 3rd solar cell and the IMS circuit board at simulated solar radiation intensities of 200, 400, 600, 800 and 1000 W/m^2, and an ambient temperature of 20 °C with forced convection along the long axis of the FPVC system.
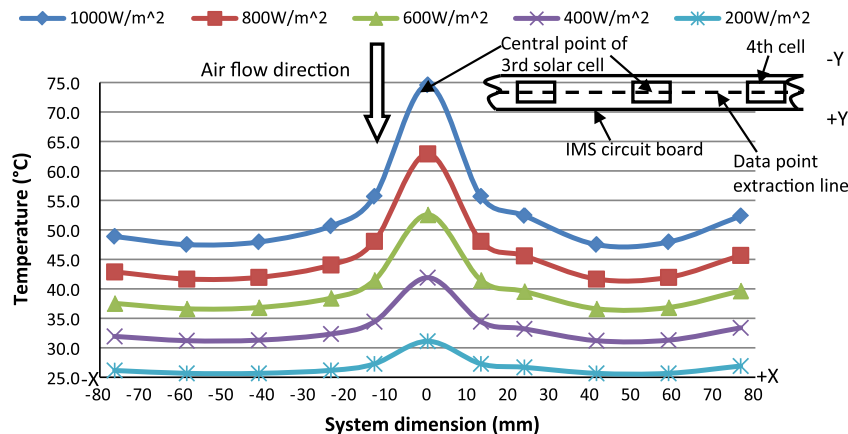
Fig. A2. Temperature distribution in the horizontal long central axis (*X*-direction) for the simulated 3rd solar cell along the IMS circuit board at simulated solar radiation intensities of 200, 400, 600, 800 and 1000 W/m², and an ambient temperature of 20 °C with forced convection over the cross section of the FPVC system.
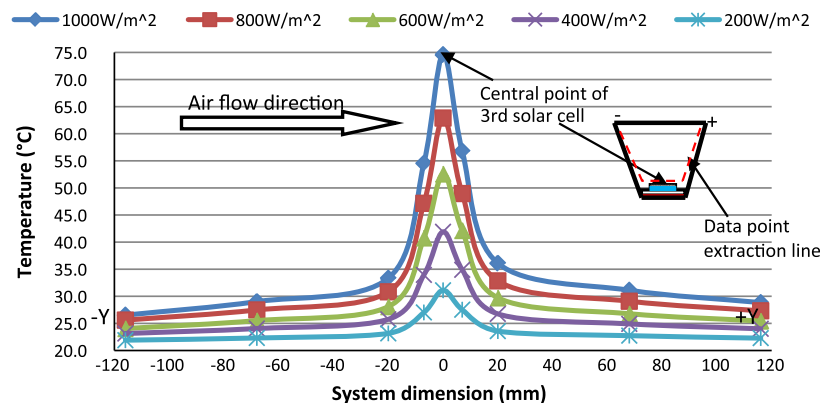

Fig. A3. Temperature distribution along the cross section for the FPVC system simulated 3rd solar cell and trough walls at simulated solar radiation intensities of 200, 400, 600, 800 and 1000 W/m², and an ambient temperature of 20 °C with forced convection over the cross section of the FPVC system.

References

Al-Jumaily, Khalil E.J., Al-Kaysi, Munadhila K.A., 1998. The study of the performance and efficiency of flat linear Fresnel lens collector with sun tracking system in Iraq. Renewable Energy 14, 41–48.

Andreev, V.M., Grilikhes, V.A., Khvostikov, V.P., Khvostikova, O.A., Rumyantsev, V.D., Sadchikov, N.A., Shvarts, M.Z., 2004. Concentrator PV modules and solar cells for TPV systems. Solar Energy Materials & Solar cells 84, 3–17.

Anon, 2005. Planning and Installing Photovoltaic Systems: A Guide for Installers, Architects and Engineers by the German Solar Energy Society (DGS). James & James, London, UK.

Anon, R.S., 2008. Data Sheet LOCTITE® 315™. RS Components, Ltd., UK.

Anon, 2009. Weather underground, <http://www.wunderground.com/global/MI.html>.

Mallick, T.K., Eames, P.C., 2007a. Optical performance predictions for a high concentration point focus photovoltaics system. In: Proceedings of ICSC-4. El Escorial, Spain.

Mallick, T.K., Eames, P.C., 2007b. Optical and thermal performance predictions for a high concentration point focus photovoltaic system. In: Proceedings of ISES. Beijing, China.

Nabelek, B., Maly, M., Jirka, V.l., 1991. Linear Fresnel lenses, their design and use. Renewable Energy 1, 403–408.

Rabl, A., 1976. Comparison of Solar Concentrators. Solar Energy 18, 93–111.

Ryu, K., Rhee, J.G., Park, K.M., Kim, J., 2006. Concept and design of modular Fresnel lenses for concentration solar PV system. Solar Energy 80, 1580–1587.

Salim, A.A., Eugenio, N.N., 1990. A comprehensive report on the performance of the longest operating 350 kW concentrator photovoltaic power system. Solar Energy 29, 1–24.

Singh, P.L., Ganesan, S., Yàdav, G.C., 1999. Performance study of a linear Fresnel concentrating solar device. Renewable Energy 18, 409–416.

Whitfield, G.R., Bentley, R.W., Weatherby, C.K., Hunt, A.C., Mohring, H.D., Klotz, F.H., Keuber, P., Minano, J.C., 1999. The development and testing of small concentrating PV system. Solar Energy 67, 23–34.

Winston, R., Miñano, J.C., Benítez, P., 2005. Nonimaging Optics. Elsevier Academic Press, London, UK.